Cationic Zirconocene and Hafnocene Aryl Complexes

Orson L. Sydora, Stefan M. Kilyanek, and Richard F. Jordan*

Department of Chemistry, The University of Chicago, 5735 South Ellis Avenue, Chicago, Illinois 60637

Received May 3, 2007

Cationic $(C_5H_4R)_2ZrAr^+$ aryl species (**2a**−**d**: R = H; Ar = *o*-tolyl (**a**), 2-Me-4-F-C_6H_3 (**b**), 3-F-C_6H_4 (**c**), Ph (**d**); **2e**: R = Me, Ar = Ph) are generated by the reaction of a 1:1 mixture of $(C_5H_4R)_2ZrAr_2$ and $(C_5H_4R)_2ZrMe_2$ with 2 equiv of $[CPh_3][B(C_6F_5)_4]$ via methide abstraction and ligand exchange steps. Complex **2d** and the Cp_2HfAr^+ analogues (**2f,g**: Ar = *o*-tolyl (**f**), Ph (**g**)) are generated by the reaction of Cp_2MAr_2 with $[C_6Me_6H][B(C_6F_5)_4]$. NMR studies suggest that these metallocene aryl cations exist as $(C_5H_4R)_2M(Ar)(RCl)^+$ solvent adducts in chlorocarbon solution. NMR and DFT studies show that the $(C_5H_4R)_2Zr(Ar)(RCl)^+$ species contain β-C−H−Zr agostic interactions involving an ortho-aryl hydrogen. The "endo" isomers, in which the β-agostic interaction occupies the central coordination site, are ca. 5 kcal/mol more stable than the "exo" isomers, in which the β-agostic interaction occupies a lateral site. The aryl agostic interactions are weaker for Hf than Zr, and $Cp_2Hf(Ph)(C_6D_5Cl)^+$ (**2g·C_6D_5Cl**) does not contain an agostic interaction.

Introduction

We recently described the synthesis of d^0 zirconocene aryl cations $[(C_5H_4R)_2Zr(C_6F_5)][B(C_6F_5)_4]$ (**A**; Chart 1; R = H, Me) by methyl abstraction from $(C_5H_4R)_2Zr(C_6F_5)Me$ using $[Ph_3C][B(C_6F_5)_4]$.[1] Complexes **A** exist as solvent adducts and contain dative *o*-CF···Zr interactions in chlorobenzene solution. **A** reacts with allyltrimethylsilane and propargyltrimethylsilane to form d^0 $(C_5H_4R)_2Zr(C_6F_5)(substrate)^+$ alkene and alkyne complexes. These unusual species are stabilized by the combination of the silyl substituent, which strengthens substrate coordination via the β-Si effect, and the poor nucleophilicity of the $-C_6F_5$ group, which inhibits insertion. We are interested in preparing d^0 $(C_5H_4R)_2M(Ar)^+$ species with modified aryl groups in order to find systems that form observable alkene or alkyne adducts and undergo insertion, since such systems may be useful mechanistic probes.

While cationic group 4 metallocene alkyl complexes have been studied extensively, analogous aryl species are less common.[2] Hlatky et al. described the zwitterionic complex Cp*$_2$-Zr^+(2-Et-5-BAr_3-C_6H_3) (**B**; Cp* = C_5Me_5; Ar = *p*-Et-Ph), which is formed by the reaction of $Cp^*_2ZrMe_2$ with $[HNMe_2Ph][BPh_4]$ to generate $Cp^*_2ZrMe^+$ followed by CH activation of the counterion.[3] More recently, we reported $[Cp^*_2Zr(\eta^2$-*C*,-*Cl*-2-Cl-$C_6H_4)][B(C_6F_5)_4]$ (**C**), which is formed by CH activation of the coordinated solvent in $[Cp^*_2Zr(Me)(ClC_6H_5)][B(C_6F_5)_4]$.[4] Protonation of Cp_2ZrPh_2 with $[HNMe_2Ph][BPh_4]$ in THF produced $[Cp_2Zr(Ph)(THF)][BPh_4]$ (**D**).[5] Piers found that abstraction of the methylene group from the "tuck-in" complex $Cp^*(\eta^5$-η^1-$C_5Me_4CH_2)ZrPh$ by $B(C_6F_5)_3$ produced the zwitterion

Chart 1

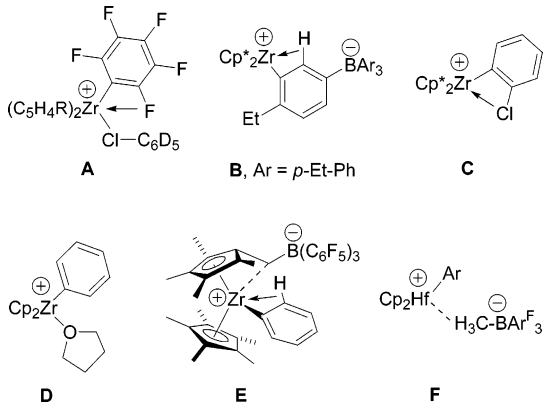

$Cp^*\{\eta^5$-$C_5Me_4CH_2B(C_6F_5)_3\}ZrPh$ (**E**).[6] $Cp_2Hf(Ar)(\mu$-Me)B-$(C_6F_5)_3$ (**F**; Ar = Ph, *o*-, *m*-, *p*-tolyl) complexes were prepared by the reaction of $Cp_2Hf(Ar)(Me)$ with $B(C_6F_5)_3$.[7]

Here we describe two routes to group 4 $(C_5H_4R)_2MAr^+$ (R = H, Me) complexes and NMR and computational studies of β-C−H aryl agostic interactions in these species.

Results and Discussion

$(C_5H_4R)_2MAr_2$ Complexes. The neutral metallocene diaryl complexes $(C_5H_4R)_2MAr_2$ (**1a**−**d**: M = Zr; R = H; Ar = *o*-tolyl (**a**), 2-Me-4-F-C_6H_3 (**b**), 3-F-C_6H_4 (**c**), Ph (**d**); **1e**: M = Zr, R = Me, Ar = Ph; **1f**,**g**: M = Hf, R = H; Ar = *o*-tolyl (**f**), Ph (**g**)) were prepared by the reaction of the corresponding metallocene dichloride with LiAr (BrMgAr for Ar = *m*-FC_6H_4).[8]

Reaction of $(C_5H_4R)_2ZrAr_2$ with $HNMePh_2^+$ or CPh_3^+. Attempts to synthesize $(C_5H_4R)_2ZrAr^+$ species by the reaction of $(C_5H_4R)_2ZrAr_2$ with $[HNMePh_2][B(C_6F_5)_4]$ or $[Ph_3C][B(C_6F_5)_4]$ were unsuccessful. The reaction of **1e** with $[HNMePh_2][B(C_6F_5)_4]$ in C_6D_5Cl did generate the Cp'_2ZrPh^+ cation (Cp′

* Corresponding author. E-mail: rfjordan@uchicago.edu.

(1) (a) Stoebenau, E. J., III; Jordan, R. F. *J. Am. Chem. Soc.* **2004**, *126*, 11170. (b) Stoebenau, E. J., III; Jordan, R. F. *J. Am. Chem. Soc.* **2006**, *128*, 8638.

(2) Cationic Organozirconium and Organohafnium Compounds. Guram, A. S.; Jordan, R. F. In *Comprehensive Organometallic Chemistry*, 2nd ed.; 1995; Vol. 4, pp 589−625.

(3) Hlatky, G. G.; Turner, H. W.; Eckman, R. R. *J. Am. Chem. Soc.* **1989**, *111*, 2728.

(4) Wu, F.; Dash, A. K.; Jordan, R. F. *J. Am. Chem. Soc.* **2004**, *126*, 15360.

(5) Borkowsky, S. L.; Jordan, R. F.; Hinch, G. D. *Organometallics* **1991**, *10*, 1268.

(6) Sun, Y.; Spence, R. E. v. H.; Piers, W. E.; Parvez, M. Yap, G. P. A. *J. Am. Chem. Soc.* **1997**, *119*, 5132.

(7) (a) Sadow, A. D.; Tilley, T. D. *J. Am. Chem. Soc.* **2002**, *124*, 6814. (b) Sadow, A. D.; Tilley, T. D. *J. Am. Chem. Soc.* **2003**, *125*, 9462.

10.1021/om700436z CCC: $37.00 © 2007 American Chemical Society
Publication on Web 08/09/2007

Scheme 1[a]

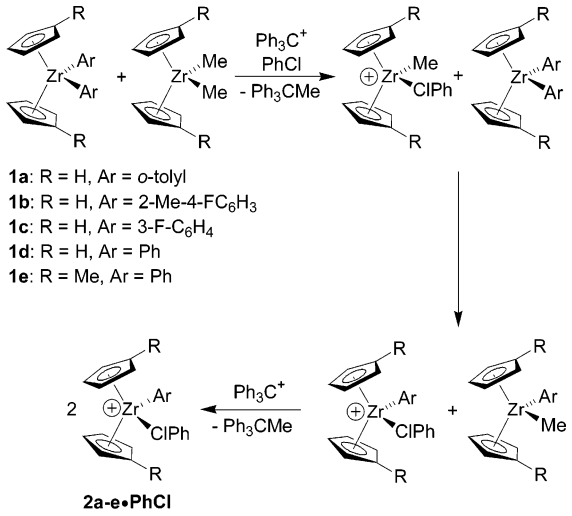

[a] Anion = $B(C_6F_5)_4^-$.

= C_5H_4Me), but it was not possible to isolate this species free of $NMePh_2$. The reaction of **1d** with $[Ph_3C][B(C_6F_5)_4]$ in chlorobenzene produced a mixture of Cp complexes, and Cp_2ZrPh^+ was not identified.

Synthesis of $(C_5H_4R)_2ZrAr^+$ by Methide Abstraction and Aryl Exchange. The potential utility of $(C_5H_4R)_2Zr(Ph)(Me)$ as a precursor to $(C_5H_4R)_2ZrPh^+$ was investigated. The reaction of $Cp'_2Zr(Me)Cl$ with 1 equiv of PhLi in Et_2O produced a mixture of $Cp'_2Zr(Ph)(Me)$ (70%), **1e** (20%), and Cp'_2ZrMe_2, from which $Cp'_2Zr(Ph)(Me)$ could not be isolated in pure form. However, the appearance of Cp'_2ZrMe_2 and **1e** in the product mixture indicates that the phenyl group can exchange between zirconocene centers under mild conditions. This observation suggested that $(C_5H_4R)_2ZrAr^+$ species might be accessible from a mixture of $(C_5H_4R)_2ZrAr_2$, $(C_5H_4R)_2ZrMe_2$, and $[Ph_3C][B(C_6F_5)_4]$ via the methide abstraction and ligand exchange process in Scheme 1.[9] Indeed, addition of an equimolar chlorobenzene solution of $(C_5H_4R)_2ZrMe_2$ and $(C_5H_4R)_2ZrAr_2$ (**1a**−**e**) to a chlorobenzene solution of 2 equiv of $[Ph_3C][B(C_6F_5)_4]$ cleanly generates $[(C_5H_4R)_2Zr(Ar)(C_6H_5Cl)][B(C_6F_5)_4]$ (**2a**−**e**•C_6H_5Cl) and Ph_3CMe as shown in Scheme 1. Compounds **2a**−**e** were isolated free of C_6H_5Cl in good yields (34−62%) as yellow solids by removal of the solvent under vacuum, washing of the resulting pale orange oil with benzene, and vacuum drying. These complexes strongly retain benzene (0.7 to 2.5 equiv) despite vacuum drying.[10]

Cations **2a**−**e** were characterized by NMR spectroscopy in CD_2Cl_2 and C_6D_5Cl solution. The ^1H and ^{13}C NMR resonances of the benzene appear at the free benzene positions, indicating that the benzene does not coordinate in solution. Two representative cases (**2a**,**d**) were also characterized by elemental analysis. Attempts to characterize these species by ESI-MS were unsuccessful due to the instability of the cation under ESI conditions. However, the reaction of **2e** with $MeC{\equiv}CSiMe_3$ yields the insertion product $Cp'_2Zr\{C(SiMe_3){=}C(Me)Ph\}^+$, which was characterized by ESI-MS and NMR.[11]

Scheme 2[a]

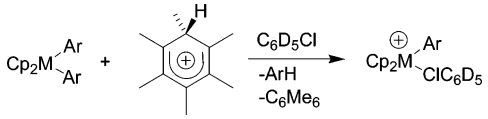

[a] Anion = $B(C_6F_5)_4^-$.

Compound **2e** is stable in C_6D_5Cl solution at 22 °C for hours in the dark, but decomposes in 12 h in the presence of light to the dinuclear complex $[\{Cp'_2Zr(\mu\text{-}Cl)\}_2][B(C_6F_5)_4]_2$, which crystallizes from solution.[12] A similar photochemical degradation was observed for $Cp_2Zr(CH_2Ph)(C_6D_5Cl)^+$ and $Cp^*_2Zr(Me)(C_6D_5Cl)^+$.[12] Complexes **2a**−**e** are far less stable in CD_2Cl_2. In this solvent, **2d** decomposes slowly at −20 °C and rapidly at room temperature to $[\{Cp_2Zr(\mu\text{-}Cl)\}_2][B(C_6F_5)_4]_2$.

Synthesis of $(C_5H_4R)_2MAr^+$ Species Using Protonated Arenes. A more straightforward route to base-free $(C_5H_4R)_2ZrAr^+$ cations is protonolysis of $(C_5H_4R)_2ZrAr_2$ complexes by protonated arenes (Scheme 2).[13] The reaction of **1d** and $[C_6Me_6H][B(C_6F_5)_4]$ (**3**) in C_6D_5Cl produces $[Cp_2M(Ph)(C_6D_5Cl)][B(C_6F_5)_4]$ (**2d**•C_6D_5Cl) cleanly. One equivalent of benzene and hexamethylbenzene are also formed in this reaction, but these arenes do not compete with the C_6D_5Cl solvent for binding to the zirconocene cation. Similarly, the reaction of **1f**,**g** and **3** in C_6D_5Cl produces $[Cp_2Hf(o\text{-tolyl})(C_6D_5Cl)][B(C_6F_5)_4]$ (**2f**•C_6D_5Cl) and $[Cp_2Hf(Ph)(C_6D_5Cl)][B(C_6F_5)_4]$ (**2g**•C_6D_5Cl). Complexes **2f**,**g**•C_6D_5Cl were characterized by NMR, but could not be isolated in pure form. The reaction of **2f**,**g**•C_6D_5Cl with $MeC{\equiv}CSiMe_3$ yields $Cp_2Hf\{C(SiMe_3){=}C(Me)Ar\}^+$ insertion products, which were characterized by ESI-MS.

C_6Me_6-Induced Degradation of Cp_2MAr^+ in CD_2Cl_2. The reaction of **1d** with **3** proceeds quite differently in CD_2Cl_2 than in C_6D_5Cl. In CD_2Cl_2 at −78 °C, this reaction results in complete consumption of the starting materials and formation of 0.5 equiv of the hexadienyl cation $[C_6Me_6(CD_2Cl)]^+$ (**4**), 0.5 equiv of $[\{Cp_2ZrPh\}_2(\mu\text{-}Cl)][B(C_6F_5)_4]$ (**5**), 0.5 equiv of C_6Me_6, and 1 equiv of benzene, as shown in Scheme 3. An analogous reaction was observed for **1g** and **3** in CD_2Cl_2 at −78 °C.

Compounds **4** and **5** were identified by NMR, ESI-MS (**4** only), and independent synthesis. The cation of **4** was synthesized as $[C_6Me_6(CD_2Cl)][Zr_2Cl_9]$ by Floriani's method.[14] Compound **5** was generated by the reaction of Cp_2ZrPh^+ (**2d**) with 0.5 equiv of $[NBu_3CH_2Ph]Cl$.

As shown in Scheme 4, the reaction in Scheme 3 likely proceeds by initial protonolysis of a M−Ph bond of **1** to yield

(8) (a) Samuel, E.; Rausch, M. D. *J. Am. Chem. Soc.* **1973**, *95*, 6263. (b) Chen, S.; Liu, Y.; Wang, *J. Sci. Sin. (Engl. Ed.)* **1982**, *25*, 341. (c) Erker, G.; Czisch, P.; Benn, R.; Rufinska, A.; Mynott, R. *J. Organomet. Chem.* **1987**, *328*, 101. (d) Tainturier, G.; Fahim, M.; Trouve-Bellan, G.; Gautheron, B. *J. Organomet. Chem.* **1989**, *376*, 321. (e) Erker, G. *J. Organomet. Chem.* **1977**, *134*, 189. (f) Chen, S.-S. *Kexue Tongbao* **1980**, *25*, 270. (g) Chen, S.-S.; Liu, Y.-Y. *Huaxue Tongbao* **1978**, *5*, 275. (h) Chen, S.-S.; Liu, Y.-Y.; Xuan, Z.-A.; Wang, Z.-K. *Huaxue Xuebao* **1980**, *38*, 497.

(9) A similar approach was used to synthesize cationic Al alkyl compounds. Korolev, A. V.; Ihara, E.; Guzei, I. A.; Young, V. G., Jr.; Jordan, R. F. *J. Am. Chem. Soc.* **2001**, *123*, 8291.

(10) (a) Attempts to use the reaction in Scheme 1 to synthesize hafnocene aryl cations were unsuccessful. (b) $Cp_2Hf(Me)(Ph)$ can be prepared free of exchange products but is not cleanly converted to Cp_2HfPh^+ by reaction with CPh_3^+.

(11) (a) Eisch, J. J.; Piotrowski, A. M.; Brownstein, S. K.; Gabe, E. J.; Lee, F. L. *J. Am. Chem. Soc.* **1985**, *107*, 7219. (b) Horton, A. D.; Orpen, A. G. *Organometallics* **1991**, *10*, 3910.

(12) Wu, F.; Jordan, R. F. *Organometallics* **2005**, *24*, 2688.

(13) (a) Reed, C. A.; Fackler, N. L. P.; Kim, K.; Stasko, D.; Evans, D. R.; Boyd, P. D. W.; Rickard, C. E. F. *J. Am. Chem. Soc.* **1999**, *121*, 6314. (b) Stasko, D.; Reed, C. A. *J. Am. Chem. Soc.* **2002**, *124*, 1148. (c) Reed, C. A.; Kim, K.; Stoyanov, E. S.; Stasko, D.; Tham, F. S.; Mueller, L. J.; Boyd, P. D. W. *J. Am. Chem. Soc.* **2003**, *125*, 1796.

(14) Musso, F.; Solari, E.; Floriani, C.; Schenk, K. *Organometallics* **1997**, *16*, 4889.

Scheme 3[a]

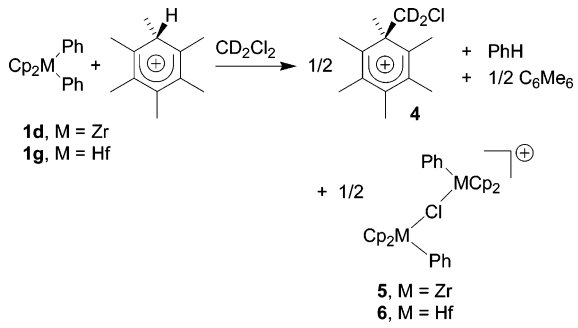

[a] Anion = $B(C_6F_5)_4^-$.

Scheme 4[a]

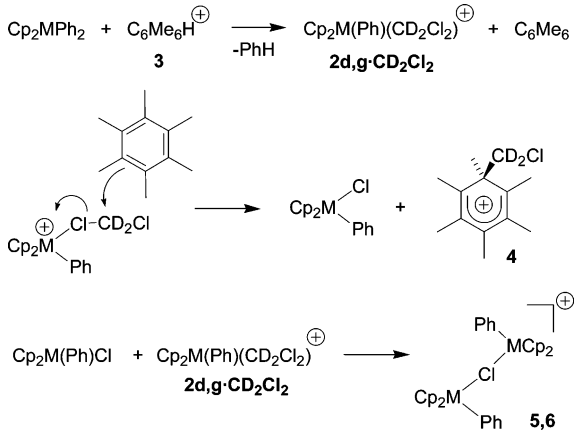

[a] M = Zr, Hf; anion = $B(C_6F_5)_4^-$.

Chart 2[a]

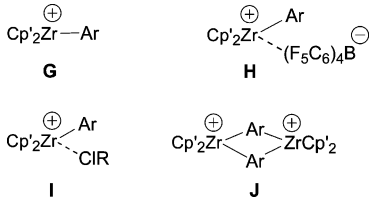

[a] Cp′ = C_5H_4Me.

2d,g·CD_2Cl_2, C_6Me_6, and benzene. Nucleophilic attack of C_6Me_6 on the CD_2Cl_2 ligand of **2d,g·CD_2Cl_2** yields $Cp_2M(Ph)Cl$ and **4**. Trapping of $Cp_2M(Ph)Cl$ by **2d,g·CD_2Cl_2** produces **5** and **6**, leaving 0.5 equiv of C_6Me_6 remaining. The reaction of independently synthesized **2d** with C_6Me_6 in CD_2Cl_2 produces **4** and **5**. However, C_6Me_6 is stable in the presence of CD_2Cl_2 and **3** for hours at room temperature.

A similar pathway was proposed for the reaction of $[(F_6\text{-acen})Zr(CH_2CMe_3)(NEt_2Ph)][B(C_6F_5)_4]$ in CD_2Cl_2.[15] In this system, nucleophilic attack of NEt_2Ph on the CH_2Cl_2 ligand of $(F_6\text{-acen})Zr(CH_2CMe_3)(CH_2Cl_2)^+$ produced $[NEt_2Ph(CH_2Cl)]^+$ and $[\{(F_6\text{-acen})Zr(CH_2CMe_3)\}_2(\mu\text{-Cl})]^+$.

Solution Structures of $(C_5H_4R)_2MAr^+$ Cations. The ^1H and ^{13}C NMR spectra of Cp'_2ZrPh^+ (**2e**) in CD_2Cl_2 at −89 °C and C_6D_5Cl at −38 °C each contain two Cp′ ring *CH* signals, consistent with C_{2v} symmetry. These data suggest four possible structures for **2e** in chlorocarbon solution (Chart 2): (i) **2e** could be a three-coordinate cation (**G**) with the aryl group occupying the central coordination site in the metallocene wedge or exchanging rapidly between the lateral sites. The isoelectronic species Cp^*_2ScPh is known.[16] (ii) **2e** may be a contact ion pair (**H**), which undergoes fast site epimerization at Zr (i.e., fast exchange of the aryl ligand and anion between the sides of the metallocene, likely mediated by the solvent). Coordination of $B(C_6F_5)_4^-$ to electrophilic Zr, Th, Sc, and Al cations is known.[17] (iii) **2e** may be a solvent adduct (**I**), which undergoes rapid site epimerization at Zr. Several closely related d^0 metal−haloarene complexes have been structurally characterized, including $Cp_2Zr(\eta^2\text{-}CH_2Ph)(ClC_6D_5)^+$ and $Cp^*_2Zr(Cl)(ClC_6D_5)^+$.[4,17b,c,18] (iv) **2e** may be a dinuclear cation with bridging aryl groups (**J**). Phenyl groups are well-known bridging groups.[19]

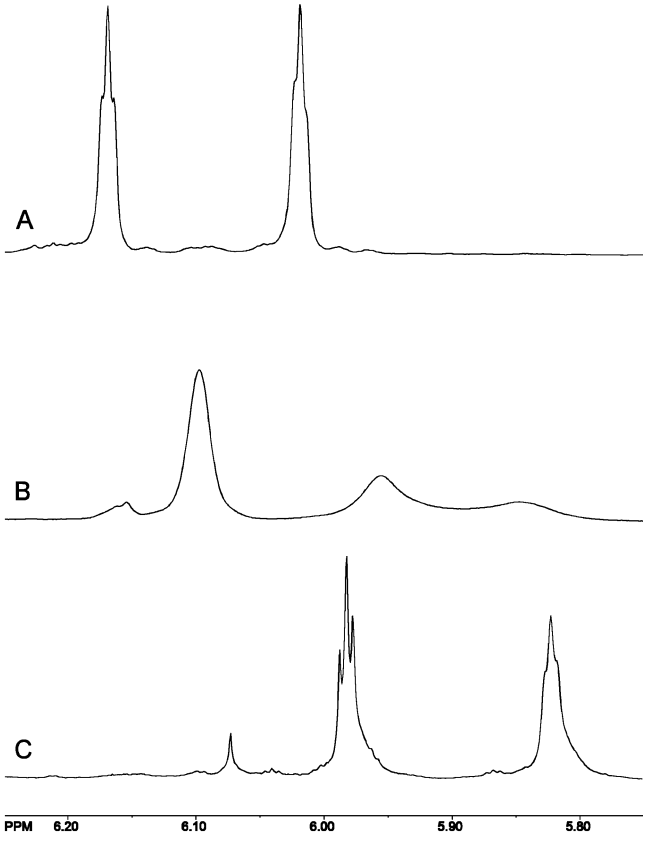

Figure 1. ^1H NMR spectra (C_5H_4Me region) of $[Cp'_2ZrPh][B(C_6F_5)_4]$ (**2e**). Spectrum A: in CD_2Cl_2 at −95 °C; spectrum B: in C_6D_5Cl/CD_2Cl_2 at −90 °C; spectrum C: in C_6D_5Cl/CD_2Cl_2 at −30 °C.

The reaction of a 1:1 mixture of **1d** and **1e** with $[C_6Me_6H][B(C_6F_5)_4]$ gives only **2d** and **2e**. No new resonances or line-broadening effects are observed in the NMR spectra of the product mixture that can be ascribed to a mixed $(C_5H_5)_2Zr(\mu\text{-}Ph)_2Zr(C_5H_4Me)_2^{2+}$ complex, which would likely form if **2d** and **2e** contained dinuclear dications. This result implies that **2d** and **2e** exist as mononuclear species in halocarbon solution and argues against **J**. The ^{19}F NMR spectrum of **2e** in CD_2Cl_2 at −89 °C contains resonances at the free anion positions, which argues against tight ion pair structure **H**.

(15) Tjaden, E. B.; Swenson, D. C.; Jordan, R. F.; Petersen, J. L. *Organometallics* **1995**, *14*, 371.

(16) Thompson, M. E.; Baxter, S. M.; Bulls, A. R.; Burger, B. J.; Nolan, M. C.; Santarsiero, B. D.; Schaefer, W. P.; Bercaw, J. E. *J. Am. Chem. Soc.* **1987**, *109*, 203.

(17) (a) Yang, X.; Stern, C. L.; Marks, T. J. *Organometallics* **1991**, *10*, 840. (b) Korolev, A. V.; Delpech, F.; Dagorne, S.; Guzei, I. A.; Jordan, R. F. *Organometallics* **2001**, *20*, 3367. (c) Bouwkamp, M. W.; Budzelaar, P. H. M.; Gercama, J.; Del Hierro Morales, I.; de Wolf, J.; Meetsma, A.; Troyanov, S. I.; Teuben, J. H.; Hessen, B. *J. Am. Chem. Soc.* **2005**, *127*, 14310.

(18) Bochmann, M.; Jaggar, A. J.; Nicholls, J. C. *Angew. Chem., Int. Ed. Engl.* **1990**, *29*, 780.

(19) (a) Koschmieder, S. U.; Wilkinson, G. *Polyhedron* **1991**, *10*, 135.

Table 1. Key NMR Data for Cationic Metallocene Aryl Species

compound	$\Delta\delta$ $H_{ortho-Ar}$[a]	$\Delta\delta$ $C_{ortho-Ar}$[a]	$J_{CH,ortho}$ (Hz)	$\Delta J_{CH,ortho}$[b]
$Cp_2Zr(o\text{-tolyl})(CD_2Cl_2)^+$ (**2a**·CD_2Cl_2)[c]	−1.1	−35.2	124	−28
$Cp_2Zr(o\text{-tolyl})(C_6D_5Cl)^+$ (**2a**·C_6D_5Cl)[d]	−1.1	−33.7	125	−27
$Cp_2Zr(2\text{-Me-4-F}-C_6H_3)(CD_2Cl_2)^+$ (**2b**·CD_2Cl_2)[c]	−1.06	−33.6	129	
$Cp_2Zr(3\text{-F}-C_6H_4)^+$ (**2c**·CD_2Cl_2)[c,g]	−0.6	−24.5	141	−16
$Cp_2ZrPh(CD_2Cl_2)^+$ (**2d**·CD_2Cl_2)[c,h]	−0.15	−15.7	147	−9
$Cp_2ZrPh(C_6D_5Cl)^+$ (**2d**·C_6D_5Cl)[d,h]	−0.47	−12.9	148	
$Cp'_2ZrPh(CD_2Cl_2)^+$ (**2e**·CD_2Cl_2)[c,h]	−0.40			
$Cp'_2ZrPh(C_6D_5Cl)^+$ (**2e**·C_6D_5Cl)[e,h]		−13.8[f]	148	−5[f]
$Cp_2Hf(o\text{-tolyl})(C_6D_5Cl)^+$ (**2f**·C_6D_5Cl)[d]	−1.26	−29.7	131	−17
$Cp_2Hf(Ph)(C_6D_5Cl)^+$ (**2g**·C_6D_5Cl)[d,i]	−0.18	−2.4	155	0

[a] $\Delta\delta = \delta$(agostic ortho-CH unit of Cp_2MAr^+) − δ(ortho-CH unit of Cp_2MAr_2). [b] $\Delta J = J$(agostic ortho-CH unit of Cp_2MAr^+) − J(ortho-CH unit of Cp_2MAr_2). [c] CD_2Cl_2, −89 °C. [d] C_6D_5Cl, 23 °C. [e] C_6D_5Cl, −38 °C. [f] Relative to data for **1e** in CD_2Cl_2 solution at −89 °C. [g] Data for the agostic CH unit (C^6-H) are listed. [h] Exchange-averaged values for the agostic and nonagostic ortho CH units. [i] Exchange-averaged values the two ortho CH units.

Chart 3

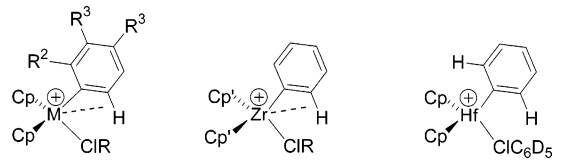

2a-d,f·RCl **2e·RCl** **2g·C_6D_5Cl**

As noted above, the ^{1}H NMR spectra of **2e** contain two Cp′ ring C*H* peaks consistent with C_{2v} symmetry in both CD_2Cl_2 and C_6D_5Cl down to −95 and −38 °C, respectively. However, as shown in Figure 1, addition of excess C_6D_5Cl to a CD_2Cl_2 solution of **2e** at −90 °C causes an increase in the number and line widths of the Cp′ C*H* resonances. When the temperature is raised to −30 °C, the signals coalesce to two peaks, which are ca. 0.25 ppm upfield from the resonances of **2e** in the absence of C_6D_5Cl at −30 °C. These results suggest that in CD_2Cl_2, **2e** exists as a solvent adduct (**2e·CD_2Cl_2**) that undergoes fast site epimerization and that addition of C_6D_5Cl results in formation of $Cp'_2Zr(Ph)(ClC_6D_5)^+$, which undergoes slow site epimerization at low temperatures and fast site epimerization at higher temperatures. Collectively, these results are most consistent with a structure of type **I** for **2e** in chlorocarbon solution. It is likely that the other $(C_5H_4R)_2MAr^+$ cations also form solvent adducts in RCl solution.

***β*-CH Agostic Interactions in $(C_5H_4R)_2M(Ar)^+$ Species.** Key NMR data for the aryl groups of **2a**−**g** in chlorocarbon solution are listed in Table 1. These data show that **2a**−**f** contain *β*-agostic interactions involving the aryl ortho C−H units, as shown in Chart 3. The key features that are characteristic of agostic interactions are high-field ortho-C−H ^{1}H and ^{13}C resonances and low $J_{CH-ortho}$ values compared to the data for the corresponding neutral $(C_5H_4R)_2MAr_2$ compounds.[20−22] For example, the aryl C^6−H ^{1}H and ^{13}C resonances of $Cp_2Zr(o\text{-tolyl})(ClCD_2Cl)^+$ (**2a·CD_2Cl_2**) are shifted upfield by 1.1 and 35.2 ppm from the corresponding resonances of **1a**, and J_{CH} for the ortho-CH unit of **2a·CD_2Cl_2** (124 Hz) is significantly reduced from the value for **1a** (152 Hz). For **2c**, the *β*-agostic interaction involves H^6, while H^2 is nonagostic.

The ^{1}H and ^{13}C spectra of the phenyl derivatives **2d**,**e** contain only single resonances for the ortho-CH units, even at low temperature, indicating that the sides of the Zr−*Ph* rings exchange rapidly. This process may occur by rotation around the Zr−Ph bond and/or by solvent-mediated site epimerization at Zr. The NMR spectra of **2e** contain one sharp ortho C−H resonance under conditions where site epimerization is apparently slow (Figure 1, spectrum B), which suggests that Zr−Ph bond rotation is fast. DFT calculations (*vide infra*) show that **2d**,**e** contain one agostic and one nonagostic ortho-CH unit. Therefore the data in Table 1 represent exchange-averaged values for one agostic and one normal ortho-C−H unit.

The data in Table 1 show that an ortho-Me substituent on the aryl ring enhances the agostic interaction of the ortho-H. For example, the J_{CH} value for the agostic CH unit in **2a·CD_2Cl_2** is reduced by 28 Hz compared to the ortho-J_{CH} value in **1a**, while J_{CH} for the agostic CH unit in **2d·CD_2Cl_2** is reduced by only 18 Hz compared to the ortho-J_{CH} value in **1d** (assuming that J_{CH} for the nonagostic ortho-CH unit in **2d·CD_2Cl_2** equals the value for **1d**).

The data in Table 1 also suggest that *β*-agostic interactions are stronger in $(C_5H_4R)_2ZrAr^+$ species than in the corresponding Hf species. For example, J_{CH} for the agostic CH in **2a·C_6D_5Cl** is lowered by 27 Hz (to 125 Hz) from the corresponding value for **1a**, while J_{CH} for the agostic CH in **2f·C_6D_5Cl** is lowered by only 17 Hz (to 131 Hz) from the value for **1f**. Moreover, while **2d·C_6D_5Cl** has one agostic CH unit, **2g·C_6D_5Cl** does not.

The agostic interactions in these systems are easily displaced by ligands. For example, the reaction of **2e** with THF yields $Cp'_2Zr(Ph)(THF)^+$ (**7**), which has a nonagostic phenyl ligand ($\Delta J_{CH,ortho} = -2$ Hz).[23] The reaction of **2d** with 1 equiv of $[NBu_3CH_2Ph]Cl$ yields $Cp_2Zr(Ph)(Cl)$ (**8**), which does not exhibit a *β*-agostic interaction ($\Delta J_{CH,ortho} = +4$ Hz).

Aryl *β*-CH agostic interactions have been observed previously in low-temperature X-ray crystal structures of metallocene aryl complexes. In **B** and **E** (Chart 1), the aryl groups lie in the plane between the Cp* ligands and exhibit distorted M−C−C bond angles indicative of *β*-CH agostic interactions. The ^{1}H NMR resonance for the ortho-CH in **B** appears at high field (δ 4.6), which is indicative of an agostic interaction. The *ansa*-metallocenes *rac*-$Me_2Si(C_5Me_4)_2Zr(Ph)Cl$ and $Me_2Si(C_5Me_4)_2$-$Zr(Ph)H$ exhibit *β*-CH agostic interactions in the solid state but not in solution.[24] NMR studies of $Cp_2Zr(CH_3)(picoline)^+$ revealed a high-field ^{1}H NMR shift and a low J_{CH} for the ortho-CH of the coordinated picoline (compared to free picoline), consistent with an agostic interaction.[22]

Computational Results. Structures of $Cp_2M(Ar)(L)^+$ Species. DFT calculations were used to probe the structures of

(20) (a) Brookhart, M.; Green, M. L. H.; Wong, L. *Prog. Inorg. Chem.* **1988**, *36*, 1. (b) Crabtree, R. H.; Hamilton, D. G. *Adv. Organomet. Chem.* **1988**, *28*, 299. (c) Cotton, F. A.; Luck, R. L. *Inorg. Chem.* **1989**, *28*, 3210. (d) Dawoodi, Z.; Green, M. L. H.; Mtetwa, V. S. B.; Prout, K.; Schultz, A. J.; Williams, J. M.; Koetzle, T. F. *J. Chem. Soc., Dalton Trans.* **1986**, 1629.

(21) Jordan, R. F.; Bradley, P. K.; Baenziger, N. C.; LaPointe, R. E. *J. Am. Chem. Soc.* **1990**, *112*, 1289.

(22) Jordan, R. F.; Taylor, D. F.; Baenziger, N. C. *Organometallics* **1990**, *9*, 1546.

(23) $\Delta J_{CH,ortho}$ = change in $J_{CH,ortho}$ compared to the corresponding $(C_5H_4R)MAr_2$ compound.

(24) (a) Lee, H.; Desrosiers, P. J.; Guzei, I.; Rheingold, A. L.; Parkin, G. *J. Am. Chem. Soc.* **1998**, *120*, 3255. (b) Lee, H.; Bridgewater, B. M.; Parkin, G. *J. Chem. Soc., Dalton Trans.* **2000**, 4490.

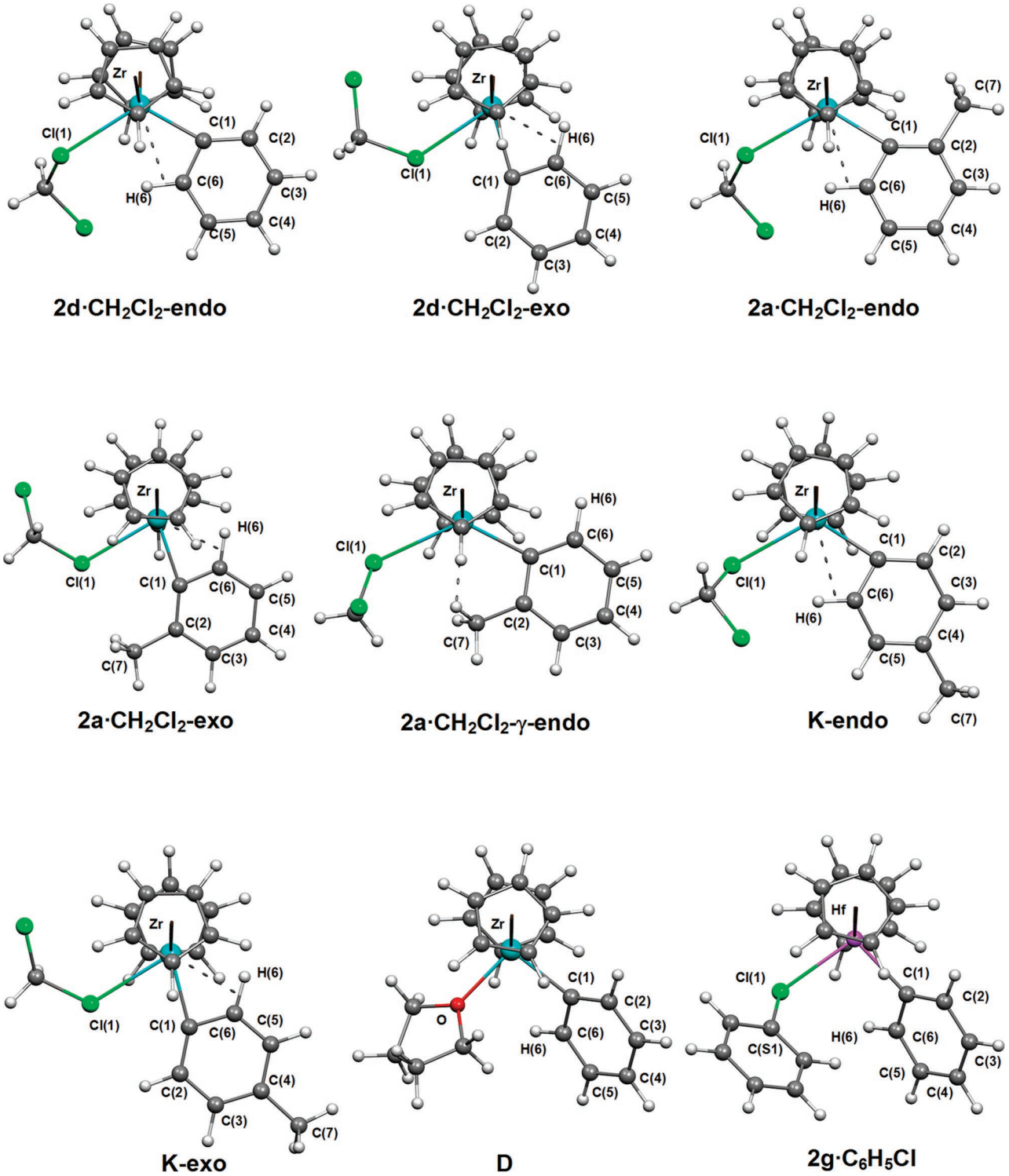

Figure 2. Calculated structures of $Cp_2M(Ar)(L)^+$ species.

$Cp_2M(Ar)(L)^+$ species and the factors that influence the β-agostic interactions in these compounds. All reasonable isomers of $Cp_2Zr(Ph)(CH_2Cl_2)^+$ (**2d·CH$_2$Cl$_2$**), $Cp_2Zr(o\text{-tolyl})(CH_2Cl_2)^+$ (**2a·CH$_2$Cl$_2$**), $Cp_2Zr(p\text{-tolyl})(CH_2Cl_2)^+$ (**K**), $Cp_2Zr(Ph)(THF)^+$ (**D**), and $Cp_2Hf(Ph)(C_6H_5Cl)^+$ (**2g·C$_6$H$_5$Cl**) were optimized. Figure 2 shows the structures that were found.

For **2d·CH$_2$Cl$_2$** and **K**, two isomers were found: an "endo" isomer in which the β-agostic interaction occupies the central coordination site, and an "exo" isomer in which the β-agostic occupies a lateral site. Three isomers were found for **2a·CH$_2$Cl$_2$**: the endo and exo β-agostic isomers and an isomer in which a γ-H-agostic interaction involving a tolyl-methyl hydrogen occupies the central coordination site (**2a·CH$_2$Cl$_2$-γ-endo**). The optimized structures of THF adduct **D** and Hf complex **2g·C$_6$H$_5$Cl** do not contain agostic interactions. Metrical parameters for the optimized structures are listed in Table 2.[25]

The β-H-agostic interactions in **2a**,**d·CH$_2$Cl$_2$** and **K** are characterized by short Zr−H(6) distances (2.21−2.48 Å), long C(6)−H(6) bond distances (1.11−1.13 Å), and small Zr−C(1)−C(6) bond angles (85−93°). Interestingly, the Zr−H(6) distance

(25) DFT structures of $Cp_2Zr(Ph)(ClC_6H_5)^+$ and $Cp_2Zr(o\text{-tolyl})(ClC_6H_5)^+$ also contain agostic interactions (see Supporting Information).

Table 2. Selected Bond Distances (Å), Bond Angles (deg), and Dihedral Angles (deg) for Cp_2MAr^+ Species

parameter	**2d·CH_2Cl_2-endo**	**2d·CH_2Cl_2-exo**	**2a·CH_2Cl_2-endo**	**2a·CH_2Cl_2-exo**	**K-endo**	**K-exo**	**D**	**2g·C_6H_5Cl**
M−H(6)	2.477	2.286	2.418	2.210	2.484	2.289	3.018	3.109
av C−H[a]	1.095	1.094	1.094	1.094	1.096	1.095	1.095	1.095
C(6)−H(6)	1.114	1.127	1.117	1.131	1.114	1.126	1.099	1.098
M−C(1)	2.205	2.232	2.209	2.242	2.201	2.222	2.264	2.259
M−C(6)	2.687	2.585	2.662	2.542	2.681	2.581	3.058	3.118
M−Cl(1)	2.842	2.807	2.858	2.812	2.846	2.795		2.703
M−O							2.279	
Cp(1)−M[b]	2.234	2.241	2.228	2.239	2.233	2.239	2.241	2.224
Cp(2)−M[b]	2.224	2.239	2.234	2.255	2.227	2.247	2.245	2.209
Cp−M−Cp[c]	131.15	131.79	131.18	130.86	130.59	131.42	128.99	131.12
M−C(1)−C(6)	93.49	87.63	91.77	85.24	93.41	87.86	109.93	113.62
C(1)−C(6)−H(6)	122.01	121.71	121.87	121.72	122.10	121.76	120.56	120.40
Cl(1)−M−C(1)	118.42	71.73	119.14	78.19	117.79	72.74		97.99
O−M−C(1							96.04	
M−Cl(1)−C(S1)								114.00
Cl(1)−M−C(1)−C(6)	−1.26	178.25	−1.42	175.44	−13.09	177.43		38.92
O−M−C(1)−C(6							42.05	
M−C(1)−C(6)−H(6)	−4.71	0.44	−5.47	0.20	−11.04	2.72	14.15	10.54

[a] The average of the bond lengths of all nonagostic aryl C−H bonds. [b] M−(Cp centroid) distance. [c] (Cp centroid)−M−(Cp centroid) angle.

Table 3. Difference in Energy between Structures with Exo and Endo Agostic Interactions

structure	$E_{structure} - E_{endo}$ (kcal/mol)[a]
2d·CH_2Cl_2-endo	0
2d·CH_2Cl_2-exo	5.4
2a·CH_2Cl_2-endo	0
2a·CH_2Cl_2-exo	6.1
2a·CH_2Cl_2-γ-endo	5.8
K-endo	0
K-exo	4.6

[a] Energy of the given species relative to that of the corresponding endo β-C−H−Zr agostic species.

is ca. 0.2 Å shorter, the C(6)−H(6) distance is ca. 0.015 Å longer, and the Zr−C(1)−C(6) angle is ca. 5.5° smaller in the exo isomers of **2a**,**d·CH_2Cl_2** and **K** compared to the endo isomers, indicating that the agostic interaction is stronger in the exo isomers than in the endo isomers.

In contrast to **2a**,**d·CH_2Cl_2** and **K**, for the nonagostic compounds **D** and **2g·C_6H_5Cl**, the M−H(6) distances are greater than 3 Å, the C(6)−H(6) bonds are not significantly lengthened, and the M−C(1)−C(6) bond angles are within 10° of the ideal sp^2 value of 120°. Additionally, while the aryl rings in **2a**,**d·CH_2Cl_2** lie in the plane between the two Cp ligands, which maximizes overlap of the ortho-C−H bonding orbital and the acceptor orbital on Zr, the phenyl rings of **D** and **2g·C_6H_5Cl** are rotated ca. 40° out of this plane.

Relative Stability of Endo and Exo Isomers. Even though the β-H agostic interaction is stronger in the exo isomers than the endo isomers of **2a**,**d·CH_2Cl_2** and **K**, the endo isomers are ca. 5 kcal/mol more stable than the exo isomers, as summarized in Table 3. One reason for this difference is that the strong agostic interaction in the exo isomers requires that the Zr−C(1)−C(6) angle be distorted to bring the C(6)−H(6) bond close to the metal, which diminishes the overlap between the C(1) and Zr bonding orbitals and weakens the Zr−C(1) bond. As shown in Table 2, the Zr−C(1) bond is 0.02−0.03 Å longer and the Zr−Cp bonds are 0.01−0.02 Å longer in the exo isomers than the endo isomers. Moreover, the exo isomers are destabilized by close contacts (<2.6 Å) between the agostic hydrogen H(6) and the Cp hydrogens.[26]

The greater stability of the endo isomers compared to the exo isomers may also be a result of the difference in donor ability of the Zr−*Ph* ligand (strong σ-donor) and the agostic *C*−*H* ligand (weak σ-donor). For group 4 metal $Cp_2M(\eta^2$-acyl)X complexes, the O-inside isomers are more stable than the O-outside isomers; that is, the complex is more stable when the stronger donor (the acyl carbon sp^2 orbital) occupies the lateral coordination site. This trend was ascribed to lowering of the HOMO energy due to greater overlap of the acyl carbon sp^2 orbital and the metal acceptor orbital in the O-inside isomer than in the O-outside isomer.[27] The greater stability of the endo isomers of β-agostic $Cp_2M(Ar)(RCl)^+$ species compared to the exo isomers is consistent with this trend.

Effect of Ortho Methyl Groups on C−H Agostic Interactions. As noted above, NMR data suggest that the aryl β-agostic interactions are enhanced by ortho-methyl groups. This result is confirmed by the calculations. As shown in Table 2, the Zr−H(6) distance is smaller, the C(6)−H(6) bond is longer, and the Zr−C(1)−C(6) angle is smaller in **2a·CH_2Cl_2** compared to the corresponding isomers of **2d·CH_2Cl_2** and **K**. The structures of **K-endo** and **K-exo**, which contain a para-methyl group, are nearly identical to those of **2a·CH_2Cl_2-endo** and **2a·CH_2Cl_2-exo**, which implies that the electron-donating effect of the methyl group does not strongly influence the strength of the β-agostic interaction. The enhanced agostic interaction in **2a·CH_2Cl_2** can be ascribed to steric crowding between the ortho methyl group and the $Cp_2Zr(CH_2Cl_2)$ unit, which forces the C(6)−H(6) bond closer to the Zr center. Similar effects were noted in zirconocene alkenyl complexes.[28]

Electronic Features of β-Agostic Interactions in $Cp_2M(Ar)(RCl)^+$ Cations. Figure 3 shows the C(6)−H(6) bonding orbital (HONLMO-46)[29] of **2a·CH_2Cl_2-endo** generated by the

(26) The steric crowding in these structures was analyzed using natural steric analysis (NSA). The NSA-determined "total steric exchange energy" of **2d·CH_2Cl_2-endo** is 2.4 kcal mol^{-1} lower than that of **2d·CH_2Cl_2-exo**, and the sum of the pairwise steric exchange energies between the C(6)−H(6) bonding orbital and the Cp_2Zr orbitals of **2d·CH_2Cl_2-endo** is 4 kcal mol^{-1} lower than that for **2d·CH_2Cl_2-exo**. These estimates sugguest that **2d·CH_2Cl_2-endo** is less crowded than **2d·CH_2Cl_2-exo**. See the Supporting Information for details. For NSA see: (a) Badenhoop, J. K.; Weinhold, F. *J. Chem. Phys.* **1997**, *107*, 5406. (b) Badenhoop, J. K.; Weinhold, F. *J. Chem. Phys.* **1997**, 107, 5422. (c) Badenhoop J. K.; Weinhold, F. *Int. J. Quantum Chem.* **1999**, *72*, 269.

(27) Tatsumi, K.; Nakamura, A.; Hofmann, P.; Stauffert, P.; Hoffmann, R. *J. Am. Chem. Soc.* **1985**, *107*, 4440.

(28) Hyla-Kryspin, I.; Gleiter, R.; Krüger, C.; Zwettler, R.; Erker, G. *Organometallics* **1990**, *9*, 517.

(29) HONLMO refers to the highest occupied natural localized molecular orbital. NLMOs are combinations of natural bonding orbitals (NBOs) obtained by analysis of the possible overlap of the NBOs in a molecule.

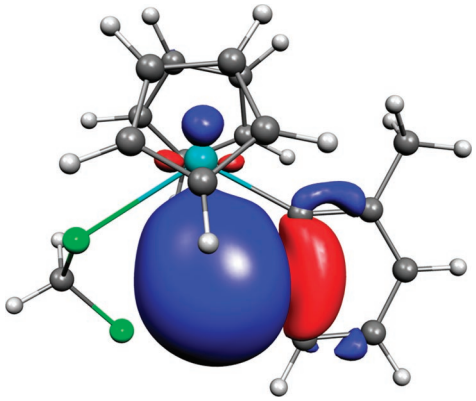

Figure 3. C(6)−H(6) NLMO (HONLMO−46) of **2a·CH$_2$Cl$_2$-endo** plotted with an iso value of 0.015 ea_0^{-3} to illustrate the 3.8% contribution from Zr.

NBO method.[30] NBO analysis shows that this NLMO has a contribution of 3.8% from the Zr (85% of which is d character). Similar results are observed for other Cp$_2$M(Ar)(RCl)$^+$ species. The C(6)−H(6) NLMOs in the exo isomers of **2a,d·CH$_2$Cl$_2$** and **K** contain a higher Zr contribution (ca. 5%) than in the endo isomers (ca. 3.5%), consistent with the relative strengths of the agostic interactions (exo > endo) implied by the calculated structures. The Zr contribution to the C(6)−H(6) NLMO is slightly (0.3%) higher in **2a·CH$_2$Cl$_2$-endo** and **2a·CH$_2$Cl$_2$-exo** compared to the corresponding isomers of **2d·CH$_2$Cl$_2$** and **K**, consistent with enhancement of the agostic interaction by the ortho methyl group.

Zr versus Hf. The NMR and computational results suggest that β-CH aryl agostic interactions are stronger in Cp$_2$Zr(Ar)(RCl)$^+$ complexes than in analogous Hf species. Differences in Zr−Ar and Hf−Ar bond strengths (Hf > Zr) may contribute to this difference.[31] The lengthening of the M−aryl bond and distortion of the M−C(2)−C(6) bond angles that accompany the agostic interaction are expected to be more difficult for Hf complexes compared to analogous Zr complexes, and as a result, agostic interactions may be less favored for Hf than Zr. In particular, for **2g·C$_6$H$_5$Cl**, the energetic cost of distorting the Hf−Ph bond may outweigh the stabilization gained by forming an agostic bond.

Differences in the Lewis acidity of the Zr and Hf species may contribute to the difference in agostic interactions, but the available data are insufficient to fully assess this issue. The equilibrium constant for coordination of pyridine to M(CH$_2$Ph)$_4$ in eq 1 is 12.6(6) M^{-1} for M = Zr and 460(30) M^{-1} for M = Hf.[32] However, differences in the benzyl coordination mode (η^1 vs η^n) complicate interpretation of this difference.

$$\mathrm{M(CH_2Ph)_4} + \mathrm{py} \overset{\mathrm{PhCl}}{\rightleftharpoons} \mathrm{M(CH_2Ph)_4(py)} \qquad (1)$$

In contrast, the reaction of a 1:1 mixture of Cp$_2$Zr(Me)(C$_6$D$_5$Cl)$^+$ and Cp$_2$Hf(Me)(C$_6$D$_5$Cl)$^+$ with <2 equiv of PMe$_3$ shows no preference for Cp$_2$Hf(Me)(PMe$_3$)$^+$ over Cp$_2$Zr(Me)(PMe$_3$)$^+$ formation. Further studies are required to quantify possible differences in the Lewis acidity of analogous Cp$_2$Zr and Cp$_2$Hf species.

Conclusions

Cationic (C$_5$H$_4$R)$_2$ZrAr$^+$ aryl species (R = H, Me) are generated by the reaction of a 1:1 mixture of (C$_5$H$_4$R)$_2$ZrAr$_2$ and (C$_5$H$_4$R)$_2$ZrMe$_2$ with [CPh$_3$][B(C$_6$F$_5$)$_4$]. Alternatively, both Zr and Hf Cp$_2$MAr$^+$ cations are generated by the reaction of Cp$_2$MAr$_2$ with [C$_6$Me$_6$H][B(C$_6$F$_5$)$_4$]. The metallocene aryl cations exist as (C$_5$H$_4$R)$_2$M(Ar)(RCl)$^+$ solvent adducts in chlorocarbon solution and generally contain β-C−H−M agostic interactions. The "endo" isomers, in which the β-agostic interaction occupies the central coordination site, are ca. 5 kcal/mol more stable than the "exo" isomers, in which the β-agostic interaction occupies a lateral site. The aryl agostic interactions are weaker for Hf than Zr, and Cp$_2$Hf(Ph)(C$_6$D$_5$Cl)$^+$ does not contain an agostic interaction.

Experimental Section

General Procedures. All manipulations were performed using drybox or Schlenk techniques under an N$_2$ atmosphere, or a high-vacuum line, unless otherwise indicated. Nitrogen was purified by passage through columns containing activated molecular sieves and Q-5 oxygen scavenger. CD$_2$Cl$_2$ and C$_6$D$_5$Cl were distilled from P$_4$O$_{10}$ and degassed prior to use. Pentane, hexane, benzene, and toluene were purified by passage through columns of activated alumina and BASF R3-11 oxygen scavenger. Cp$_2$ZrPh$_2$,[8a] Cp′$_2$ZrPh$_2$,[8b] Cp$_2$HfPh$_2$,[8a] Cp$_2$Zr(*o*-tolyl)$_2$,[8c] and Cp$_2$Hf(*o*-tolyl)$_2$[8d] were prepared by literature procedures. NMR data for these compounds are listed below. All other chemicals were purchased from Aldrich and used as received. Elemental analyses were performed by Midwest Microlab (Indianapolis, IN).

NMR spectra were recorded on Bruker DMX-500 or DRX-400 spectrometers in Teflon-valved tubes at ambient probe temperature unless otherwise indicated. ^{1}H and ^{13}C chemical shifts are reported versus SiMe$_4$ and were determined by reference to the residual solvent signals. Coupling constants are reported in Hz. For cases in which ^{13}C{gated-^{1}H} NMR spectra are reported, ^{13}C{^{1}H} NMR spectra were also recorded to assist in interpretation. For cases in which J_{HF} values are reported, ^{1}H{^{19}F} NMR spectra were collected to independently determine J_{HH} values.

The NMR spectra of ionic compounds contain resonances for the free B(C$_6$F$_5$)$_4^-$ anion. ^{19}F NMR spectra were obtained for all compounds that contain this anion. Data for B(C$_6$F$_5$)$_4^-$: ^{13}C{^{1}H} NMR (C$_6$D$_5$Cl, 23 °C) δ 148.9 (d, $^1J_{CF}$ = 242), 138.8 (d, $^1J_{CF}$ = 245), 136.9 (d, $^1J_{CF}$ = 245), 124.4 (br m); ^{13}C{^{1}H} NMR (C$_6$D$_5$Cl, −38 °C) δ 148.9 (d, $^1J_{CF}$ = 240), 138.8 (d, $^1J_{CF}$ = 236), 136.9 (d, $^1J_{CF}$ = 241), 124.7 (br m); ^{13}C{^{1}H} NMR (CD$_2$Cl$_2$, −89 °C) δ 147.1 (d, $^1J_{CF}$ = 244), 137.4 (d, $^1J_{CF}$ = 242), 135.5 (d, $^1J_{CF}$ = 243), 122.5 (br m); ^{19}F{^{1}H} NMR (C$_6$D$_5$Cl, 23 °C) δ −131.7 (br s, 8F, *o*-F), −161.8 (t, *J* = 21, 4F, *p*-F), −165.9 (br t, 8F, *m*-F); ^{19}F{^{1}H} NMR (C$_6$D$_5$Cl, −38 °C) δ −132.0 (br d, 8F, *o*-F), −161.4 (t, *J* = 20, 4F, *p*-F), −165.4 (br t, 8F, *m*-F); ^{19}F{^{1}H} NMR (CD$_2$Cl$_2$, −89 °C) δ −133.7 (s, 8F, *o*-F), −162.5 (t, *J* = 19, 4F, *p*-F), −166.5 (br t, 8F, *m*-F).

Electrospray mass spectra (ESI-MS) were recorded on freshly prepared samples (ca. 1 mg/mL in CH$_2$Cl$_2$) using an Agilent 1100 LC-MSD spectrometer incorporating a quadrupole mass filter with an *m*/*z* range of 0−3000. A 5 μL sample was injected by flow injection using an autosampler. Purified nitrogen was used as the nebulizing and drying gas. Typical instrumental parameters: drying gas temperature 350 °C, nebulizer pressure 35 psi, drying gas flow 12.0 L/min, fragmentor voltage 0 or 70 V. In all cases where assignments are given, the observed isotope patterns closely

(30) Glendening, E. D.; Badenhoop, J. K.; Reed, A. E.; Carpenter, J. E.; Bohmann, J. A.; Morales, C. M.; Weinhold, F. *NBO 5.0*; Theoretical Chemistry Institute, University of Wisconsin: Madison, WI, 2001; http://www.chem.wisc.edu/~nbo5.

(31) (a) Chase, M. W., Jr.; Davies, C. A.; Dome, J. R., Jr.; Frurip, D. J.; McDonald, R. A.; Syverud, A. N. JANAF Thermo-chemical Tables, 3rd ed. *J. Phys. Chem. Ref. Data* **1985**, *14*, Suppl. 1. (b) Schock, L. E.; Marks, T. J. *J. Am. Chem. Soc.* **1988**, *110*, 7701. (c) Martinho Simões, J. A.; Beauchamp, J. L. *Chem. Rev.* **1990**, *90*, 629.

(32) Felten, J. J.; Anderson, W. P. *J. Organomet. Chem.* **1972**, *36*, 87.

matched calculated isotope patterns. The listed *m*/*z* value corresponds to the most intense peak in the isotope pattern.

Complexes **2a**−**g** were shielded from light when handled in solution, and CD_2Cl_2 solutions of **2a**−**e** were freshly made and kept at temperatures below −60 °C.

$Cp_2Zr(o\text{-tolyl})_2$ (1a). ^{1}H NMR (CD_2Cl_2): δ 7.15 (d, J = 7, 2H, H3 or H6), 7.05 (d, J = 7, 2H, H3 or H6), 6.96 (m, 4H, H4 and H5), 6.12 (s, 10H, Cp), 2.35 (s, 6H, Me). ^{1}H NMR (C_6D_5Cl) key data: δ 7.2 (m, H3 and H6, 2H), 6.82 (s, 10H, Cp). ^{13}C{gated-^{1}H} NMR (CD_2Cl_2, −89 °C): δ 182.1 (s, C1), 145.9 (s, C2), 129.0 (d, J = 152, C6), 128.4 (d, J = 154), 124.7 (d, J = 159), 122.3 (d, J = 160), 110.3 (d, J = 174, Cp), 25.4 (q, J = 125, Me). ^{13}C{gated-^{1}H} NMR (C_6D_5Cl) key data: δ 129.6 (d, J = 152, C6), 111.8 (d, J = 173, Cp).

$Cp_2Zr(2\text{-Me-4-F-}C_6H_3)_2$ (1b). A flask was charged with 2-bromo-5-fluorotoluene (1.05 g, 5.53 mmol), and a sidearm addition tube containing Cp_2ZrCl_2 (0.812 g, 2.78 mmol) was attached. Diethyl ether (20 mL) was added, the solution was stirred at 23 °C, and ^{n}BuLi (2.1 mL, 2.68 M in hexane, 5.63 mmol) was added dropwise. After 30 min, the Cp_2ZrCl_2 was added slowly to the pale yellow solution and the mixture was stirred for 1.5 h. The solvent was removed under vacuum, yielding a yellow-white solid. This material was taken up in toluene (ca. 10 mL) and filtered to give a yellow filtrate. The filtrate was concentrated under vacuum until the saturation point was reached. Hexane was layered onto the solution, precipitating a white microcrystalline solid. A second recrystallization using the same procedure yielded analytically pure product (0.18 g, 15%). ^{1}H NMR (CD_2Cl_2, 23 °C): δ 7.02 (dd, $^3J_{HH}$ = 8.2, $^4J_{HF}$ = 7.2, 2H, H6), 6.78 (dd, $^3J_{HF}$ = 11.5, $^4J_{HH}$ = 2.3, 2H, H3), 6.67 (ddd, $^3J_{HF}$ = 9.2, $^3J_{HH}$ = 8.2, $^4J_{HH}$ = 2.5, 2H, H5), 6.14 (s, 10H, Cp), 2.30 (s, 6H, Me). ^{13}C{^{1}H} NMR (CD_2Cl_2, 23 °C): δ 175.8 (s, C1), 162.3 (d, $^1J_{CF}$ = 243, C4), 148.4 (br s, C2), 131.3 (br s, C6), 116.1 (d, $^2J_{CF}$ = 16, C3 or C5), 111.7 (br s, Cp), 109.8 (d, $^2J_{CF}$ = 18, C5 or C3), 26.1 (s, Me). ^{19}F{^{1}H} NMR (CD_2Cl_2, 23 °C): δ −119.2 (s). Anal. Calcd for $C_{24}H_{22}F_2Zr$: C, 65.56; H, 5.04. Found: C, 65.29; H, 5.04.

$Cp_2Zr(3\text{-F-}C_6H_4)_2$ (1c). A flask was charged with a THF solution of 3-fluorophenylmagnesium bromide (15.0 mL, 7.50 mmol). The solvent was removed under vacuum to afford a colorless oil, and Cp_2ZrCl_2 (1.05 g, 3.59 mmol) was added. Diethyl ether (20 mL) was added by vacuum transfer, and the mixture was stirred for 2 h at room temperature, producing a suspension of a white precipitate in a pale yellow supernatant. The volatiles were removed under vacuum, and the white solid was triturated with hexane (ca. 15 mL). The solid was taken up in toluene and filtered, and the filtrate was concentrated under vacuum. The concentrated solution was layered with hexane at −35 °C, yielding **1c** as a white, microcrystalline solid (0.35 g, 24%). ^{1}H NMR (CD_2Cl_2): δ 7.12 (td, $^3J_{HH}$ = 8, $^4J_{HF}$ = 6, 2H, H5), 6.96 (m, 4H, H2 and H6), 6.71 (t, $^3J_{HF}$ = 9, $^3J_{HH}$ = 8, 2H, H4), 6.22 (s, 10H, Cp). ^{13}C{gated-^{1}H} (CD_2Cl_2, −89 °C): δ 184.8 (s, C1), 160.8 ($^1J_{CF}$ = 249, C3), 130.2 (dd, $^1J_{CH}$ = 157, $^4J_{CF}$ = 3, C6), 127.1 (dd, $^1J_{CH}$ = 161, $^3J_{CF}$ = 5, C5), 121.8 (dd, $^1J_{CH}$ = 159, $^2J_{CF}$ = 15, *C*2), 112.3 (d, $^1J_{CH}$ = 174, Cp), 111.3 (dd, $^1J_{CH}$ = 165, $^2J_{CF}$ = 21, C4). The ^{1}H and ^{13}C assignments were confirmed by HMQC. ^{19}F{^{1}H} (CD_2Cl_2, −89 °C): δ −116.3 (s).

Cp_2ZrPh_2 (1d). ^{1}H NMR (CD_2Cl_2, −89 °C): δ 7.20 (d, J = 6.6, 4H, *o*-Ph), 7.05 (t, J = 7.2, 4H, *m*-Ph), 6.96 (t, J = 6.2, 2H, *p*-Ph), 6.17 (s, 10H, Cp). ^{1}H NMR (C_6D_5Cl): δ 7.30 (d, J = 7.2, 4H, *o*-Ph), 7.17 (t, J = 7.3, 4H, *m*-Ph), 7.07 (t, J = 6.6, 2H, *p*-Ph), 5.91 (s, 10H, Cp). ^{13}C{gated-^{1}H} (CD_2Cl_2, −89 °C): δ 182.2 (*ipso*-Ph), 135.5 (d, J = 156, *o*-Ph), 125.8 (d, J = 160, *m*-Ph), 124.6 (d, J = 159, *p*-Ph), 111.9 (d, J = 174, Cp). ^{13}C{^{1}H} (C_6D_5Cl): δ 183.1 (*ipso*-Ph), 135.8 (*o*-Ph), 126.8 (*m*-Ph), 125.5 (*p*-Ph), 112.2 (Cp).

Cp'_2ZrPh_2 (1e). ^{1}H NMR (CD_2Cl_2, −89 °C): δ 7.27 (d, J = 6.7, 4H, *o*-Ph), 7.10 (t, J = 7.2, 4H, *m*-Ph), 7.02 (t, J = 7.1, 2H, *p*-Ph), 6.15 (m, 4H, Cp′ CH), 5.91 (m, 4H, Cp′ CH), 1.69 (s, 6H, Cp′ Me). ^{13}C{gated-^{1}H} (CD_2Cl_2, −89 °C): δ 183.9 (s, *ipso*-Ph), 135.6 (d, J = 153, *o*-Ph), 125.6 (d, J = 157, *m*-Ph), 124.5 (d, J = 160, *p*-Ph), 123.4 (s, Cp′ *ipso*), 113.5 (d, J = 170, Cp′ CH), 110.2 (d, J = 172, Cp′ CH), 14.7 (q, J = 128, Cp′ Me).

$Cp_2Hf(o\text{-tolyl})_2$ (1f). ^{1}H NMR (C_6D_5Cl, 23 °C): δ 7.16 (br s, 2H, H3 or H6), 7.12 (br d, J = 7.0, 2H, H3 or H6), 7.08 (t, J = 7.3, 2H, H4 or H5), 7.02 (t, J = 7.5, 2H, H4 or H5), 5.85 (br s, 10H, Cp), 2.19 (br s, 6H, Me). ^{13}C{^{1}H} NMR (C_6D_5Cl, 23 °C): δ 190.9 (C1), 146.5 (C2), 133.0 (C6; J_{CH} = 148 Hz from ^{13}C{gated-^{1}H} spectrum at 90 °C), 130.5 (C3), 127.8 (C4), 125.6 (C5), 111.0 (Cp), 26.5 (Me). All of the ^{13}C signals are broad due to restricted rotation of the *o*-tolyl groups.

Cp_2HfPh_2 (1g). ^{1}H NMR (C_6D_5Cl, 23 °C): δ 7.35 (d, J = 7.2, 4H, *o*-Ph), 7.23 (t, J = 7.4, 4H, *m*-Ph), 7.06 (t, J = 7.3, 2H, *p*-Ph), 5.89 (s, 10H, Cp). ^{13}C{gated-^{1}H} NMR (C_6D_5Cl, 23 °C): δ 191.9 (s, *ipso*-Ph), 137.6 (d, J = 155, *o*-Ph), 127.2 (d, J = 161, *m*-Ph), 125.3 (d, J = 163, *p*-Ph), 111.9 (d, J = 177, Cp).

$[Cp_2Zr(o\text{-tolyl})][B(C_6F_5)_4]$ (2a). A chlorobenzene solution (3 mL) of $Cp_2Zr(o\text{-tolyl})_2$ (100 mg, 0.248 mmol) and Cp_2ZrMe_2 (62.3 mg, 0.248 mmol) was added dropwise to a chlorobenzene solution (5 mL) of $[Ph_3C][B(C_6F_5)_4]$ (457 mg, 0.495 mmol) in the dark. The mixture was stirred for 30 min at 23 °C. The volatiles were removed under vacuum, and the resulting orange oil was washed with benzene (3 × 5 mL) to remove triphenylethane. The orange oil was dried under vacuum, yielding $[Cp_2Zr(o\text{-tolyl})][B(C_6F_5)_4]\cdot(C_6H_6)_{1.5}$ as an orange solid (0.28 g, 53%). The benzene content was determined by NMR. ^{1}H NMR (CD_2Cl_2, −89 °C): δ 7.35 (t, J = 7.5, 1H, aryl), 7.19 (m, 2H, aryl), 6.27 (s, 10H, Cp), 6.02 (d, J = 7.3, 1H, H6), 2.32 (s, 3H, Me). ^{1}H NMR (C_6D_5Cl) key data: δ 5.9 (d, J = 7, 1H, H6), 5.74 (s, 10H, Cp). ^{13}C{gated-^{1}H} NMR (CD_2Cl_2, −89 °C): δ 192.3 (s, C1), 145.2 (s, C2), 130.6 (d, J = 159), 128.9 (d, J = 159), 126.6 (poorly resolved d, C5), 112.6 (d, J = 177, Cp), 93.8 (dd, J = 124, 9, C6), 22.8 (qd, J = 125, 4, Me). ^{13}C{gated-^{1}H} NMR (C_6D_5Cl) key data: δ 113.5 (d, J = 76, Cp), 95.9 (dd, J = 125, 10; C6). A sample of **2a** for elemental analysis was further dried under vacuum for 3 days, yielding material containing 0.7 equiv of C_6H_6 as determined by NMR. Anal. Calcd for $C_{41}H_{17}BF_{20}Zr\cdot(C_6H_6)_{0.7}$: C, 51.79; H, 2.03. Found: C, 51.82; H, 2.31.

$[Cp_2Zr(2\text{-Me-4-F-}C_6H_3)][B(C_6F_5)_4]$ (2b). This compound was prepared from $Cp_2Zr(2\text{-Me-4-F-}C_6H_3)_2$ (150 mg, 0.341 mmol), Cp_2ZrMe_2 (85.8 mg, 0.341 mmol), and $[Ph_3C][B(C_6F_5)_4]$ (629 mg, 0.682 mmol) using the procedure for **2a**. The orange oil was dried under vacuum, yielding $[Cp_2Zr(2\text{-Me-4-F-}C_6H_3)][B(C_6F_5)_4]\cdot(C_6H_6)_{1.8}$ as an orange solid (0.54 g, 34%). ^{1}H NMR (CD_2Cl_2, −89 °C): δ 6.97 (m, 2H, H3 and H4), 6.31 (s, 10H, Cp), 5.96 (dd, $^3J_{HH}$ = 7.8, $^4J_{HF}$ = 4.0, 1H, H6), 2.32 (s, 3H, Me). ^{13}C{gated-^{1}H} NMR (CD_2Cl_2, −89 °C): δ 186.3 (s, C1), 162.5 (d, $^1J_{CF}$ = 247, C4), 147.8 (d, $^3J_{CF}$ = 6, C2), 118.1 (dd, $^1J_{CH}$ = 156, $^2J_{CF}$ = 20, C3), 113.0 (d, $^1J_{CH}$ = 176, Cp), 112.1 (dd, $^1J_{CH}$ = 162, $^2J_{CF}$ = 21, C5), 97.7 (dd, $^1J_{CH}$ = 129, $^3J_{CF}$ = 10, C6), 23.0 (q, $^1J_{CH}$ = 127, Me). ^{19}F{^{1}H} (CD_2Cl_2, −89 °C): δ −114.6 (s).

$[Cp_2Zr(3\text{-F-}C_6H_4)][B(C_6F_5)_4]$ (2c). This compound was prepared from $Cp_2Zr(2\text{-F-}C_6H_4)_2$ (0.100 g, 0.243 mmol), Cp_2ZrMe_2 (0.061 g, 0.243 mmol), and $[Ph_3C][B(C_6F_5)_4]$ (0.448 g, 0.486 mmol) using the procedure for **2a**. The orange oil was dried under vacuum, yielding $[Cp_2Zr(3\text{-F-}C_6H_4][B(C_6F_5)_4]\cdot(C_6H_6)_{1.5}$ as an orange solid (0.24 g, 43%). ^{1}H NMR (CD_2Cl_2, −89 °C): δ 7.40 (td, $^3J_{HH}$ = 8, $^4J_{HF}$ = 5, 1H, H5), 7.19 (d, $^3J_{HF}$ = 7, 1H, H2), 6.93 (td, $^3J_{HH}$ = $^3J_{HF}$ = 8, $^4J_{HH}$ = 2, 1H, H4), 6.42 (s, 10H, Cp), 6.37 (d, $^3J_{HH}$ = 8, 1H, H6). ^{13}C{gated-^{1}H} (CD_2Cl_2, −89 °C): δ 193.4 (s, C1), 162.4 (d, $^1J_{CF}$ = 256, C3), 130.3 (dd, $^1J_{CH}$ = 164, $^3J_{CF}$ = 6, C5), 120.2 (dd, $^1J_{CH}$ = 163, $^2J_{CF}$ = 18, C2), 115.6 (dd, $^1J_{CH}$ = 165, $^2J_{CF}$ = 23, C4), 114.4 (d, $^1J_{CH}$ = 176, Cp), 105.7 (d, $^1J_{CH}$ = 141, C6). ^{19}F{^{1}H} (CD_2Cl_2, −89 °C): δ −112.0 (s).

$[Cp_2ZrPh][B(C_6F_5)_4]$ (2d). This compound was prepared from Cp_2ZrPh_2 (74.9 mg, 0.199 mmol), Cp_2ZrMe_2 (50.1 mg, 0.199

mmol), and $[Ph_3C][B(C_6F_5)_4]$ (367 mg, 0.398 mmol) using the procedure for **2a**. The pale orange oil was dried under vacuum, yielding $[Cp_2ZrPh][B(C_6F_5)_4]\cdot(C_6H_6)_{2.3}$ as a pale yellow solid (0.289 g, 62%). ^{1}H NMR (CD_2Cl_2, −89 °C): δ 7.39 (t, J = 7.5, 2H, *m*-Ph), 7.24 (t, J = 7.3, 1H, *p*-Ph), 7.05 (d, J = 7.5, 2H, *o*-Ph), 6.36 (s, 10H, Cp). ^{13}C{gated-^{1}H} (CD_2Cl_2, −89 °C): δ 193.0 (s, *ipso*-Ph), 129.2 (d, J = 161, *m*-Ph), 128.4 (d, J = 162, *p*-Ph), 119.8 (d, J = 147, *o*-Ph), 113.7 (d, J = 177, Cp). A sample of the product for elemental analysis was further dried under vacuum for 3 days, yielding material containing 1.3 equiv of C_6H_6 as determined by NMR. Anal. Calcd for $C_{40}H_{15}BF_{20}Zr\cdot(C_6H_6)_{1.3}$: C, 53.30; H, 2.14. Found: C, 53.24; H, 2.27.

Generation of $[Cp_2Zr(Ph)(ClC_6D_5)][B(C_6F_5)_4]$ (2d·C_6D_5Cl). An NMR tube was charged with Cp_2ZrPh_2 (15.0 mg, 0.0399 mmol) and $[C_6Me_6H][B(C_6F_5)_4]$ (33.6 mg, 0.0399 mmol), and C_6D_5Cl (0.6 mL) was added by vacuum transfer at −196 °C. The tube was warmed to 23 °C with vigorous agitation, resulting in an orange solution. NMR analysis after 15 min at 23 °C showed that clean formation of **2d·C_6D_5Cl**, 1 equiv benzene, and 1 equiv of C_6Me_6 had occurred. ^{1}H NMR (C_6D_5Cl, 23 °C): δ 7.2 (t, J = 8, 2H, *m*-Ph), 7.11 (t, J = 7.2, 1H, *p*-Ph), 6.83 (d, J = 7.2, 2H, *o*-Ph), 5.80 (s, 10 H, Cp). ^{13}C{gated-^{1}H} NMR (C_6D_5Cl, 23 °C): δ 193.1 (s, *ipso*-Ph), 122.9 (d, J = 148, *o*-Ph), 114.8 (d, J = 177, Cp); the *m*-Ph and *p*-Ph resonances are obscured by the solvent peaks.

$[Cp'_2ZrPh][B(C_6F_5)_4]$ (2e). This compound was prepared from Cp'_2ZrPh_2 (0.151 g, 0.374 mmol), Cp'_2ZrMe_2 (0.104 g, 0.372 mmol), and $[Ph_3C][B(C_6F_5)_4]$ (0.685 g, 0.743 mmol) using the procedure for **2a**. The orange oil was dried under vacuum, yielding $[Cp'_2ZrPh][B(C_6F_5)_4]\cdot(C_6H_6)_{2.0}$ as an orange solid (0.31 g, 36%). ^{1}H NMR (CD_2Cl_2, −89 °C): δ 7.45 (t, J = 7.5, 2H, *m*-Ph), 7.26 (t, J = 7.5, 1H, *p*-Ph), 6.87 (d, J = 7.3, 2H, *o*-Ph), 6.18 (m, 4H, Cp′ CH), 6.03 (m, 4H, Cp′ CH), 1.53 (s, 6H, Me). ^{1}H NMR (C_6D_5Cl, −38 °C): δ 7.24 (t, J = 7.5, 2H, *m*-Ph), 7.13 (t, J = 7.5, 1H, *p*-Ph), 6.68 (d, J = 7.1, 2H, *o*-Ph), 5.67 (m, 4H, Cp′ CH), 5.49 (m, 4H, Cp′ CH), 1.25 (s, 6H, Me). ^{13}C{gated-^{1}H} NMR (C_6D_5Cl, −38 °C): δ 194.9 (s, *ipso*-Ph), 130.3 (t, $^2J_{CH}$ = 5, Cp′ ipso), 129.6 (coupling obscured by solvent peak, *m*-Ph), 128.5 (coupling obscured by solvent peak, *p*-Ph), 121.8 (d, J = 148, *o*-Ph), 116.6 (d, J = 177, Cp′ CH), 111.3 (d, J = 177, Cp′ CH), 14.1 (q, J = 129, Me). The ^{13}C NMR assignments of **2e** were confirmed by a ^{1}H−^{13}C HMQC spectrum.

Generation of $[Cp'_2Zr\{C(SiMe_3)=C(Me)Ph\}][B(C_6F_5)_4]$. An NMR tube was charged with **2e** (12.0 mg, 0.0105 mmol), and C_6D_5Cl (0.6 mL) was added by vacuum transfer at −196 °C. The tube was warmed to 23 °C and shaken vigorously, giving a yellow solution. The tube was cooled to −196 °C, and $MeC{\equiv}CSiMe_3$ (0.0714 mmol) was added by vacuum transfer. The tube was warmed to −36 °C, giving a pale orange solution. The tube was transferred to a precooled NMR probe (−38 °C), and NMR spectra showed that the insertion reaction was complete. ^{1}H NMR (C_6D_5Cl, −38 °C): δ 7.08 (t, J = 7.3, 1H, aryl), 7.05 (d, J = 6.5, 2H, aryl), 6.96 (t, J = 7.3, 2H, aryl), 5.86 (m, 2H, Cp′ CH), 5.57 (m, 2H, Cp′ CH), 5.31 (m, 2H, Cp′ CH), 5.27 (m, 2H, Cp′ CH), 1.85 (s, 3H ═C*Me*), 1.83 (s, 6H, Cp′ Me), −0.08 (s, 9H, ═CSi*Me*$_3$). ^{13}C{^{1}H} NMR (C_6D_5Cl, −35 °C): δ 214.0, 149.1, 146.4, 137.0, 131.8, 131.7, 117.6 (Cp′), 116.9 (Cp′), 115.9 (Cp′), 115.3 (Cp′), 112.7, 26.0 (═C*Me*), 15.1 (Cp′*Me*), 1.3 (═CSi*Me*$_3$). ESI-MS (C_6D_5Cl) $[Cp'_2Zr(C(SiMe_3){=}CMePh]^+$: calcd m/z 437.1, found 437.0.

$[C_6Me_6H][B(C_6F_5)_4]$ (3). This compound was prepared using the method developed by Reed for $[H(mesitylene)][B(C_6F_5)_4]$ and $[H(tetramethylbenzene)][B(C_6F_5)_4]$.[13] A glass vial was silylated by treatment with a solution containing Me_3SiCl and CH_2Cl_2 (1:3 volume ratio) for 5 min followed by an acetone rinse and oven drying for 12 h. The vial was charged with $[Ph_3C][B(C_6F_5)_4]$ (0.242 g, 0.262 mmol) and triethylsilane (3 mL). The mixture was stirred overnight, and the volatiles were removed under vacuum. The resulting white solid was washed with hexane (2 × 5 mL) and dried under vacuum. Hexamethylbenzene (40.1 mg, 0.247 mmol) was added to the vial, and the solids were dissolved in toluene (3 mL). Triflic acid (5 drops, ca. 0.5 mmol) was added, producing a yellow oil. Hexane (5 mL) was added, and a yellow solid rapidly precipitated. The solid was recrystallized two times by layering hexane onto toluene solutions to produce spectroscopically pure product (0.15 g, 66%). ^{1}H NMR (CD_2Cl_2, −89 °C): δ 3.96 (br s, 1H), 2.69 (s, 3H), 2.54 (s, 6H), 2.22 (s, 6H), 1.52 (d, J = 7.8, 3H). ^{13}C{^{1}H} NMR (CD_2Cl_2, −89 °C): δ 192.8, 190.8, 139.1, 57.1, 24.3 (2C), 21.0, 15.4. ESI-MS (C_6D_5Cl) $[C_6Me_6H]^+$: calcd m/z 163.2, found 163.1.

Generation of $[Cp_2Hf(o\text{-tolyl})(ClC_6D_5)][B(C_6F_5)_4]$ (2f·C_6D_5Cl). An NMR tube was charged with $Cp_2Hf(o\text{-tolyl})_2$ (35.1 mg, 0.0712 mmol) and $[C_6Me_6H][B(C_6F_5)_4]$ (60.0 mg, 0.0712 mmol), and C_6D_5Cl was added by vacuum transfer at −196 °C. The tube was warmed to 23 °C and vigorously agitated, resulting in a pale yellow solution. NMR analysis after 15 min at 23 °C showed that clean formation of **2f·C_6D_5Cl**, 1 equiv of toluene, and 1 equiv of C_6Me_6 had occurred. Data for **2f·C_6D_5Cl**: ^{1}H NMR (C_6D_5Cl, 23 °C): δ 7.19 (t, J = 7.2, 1H, H4 or H5), 7.09 (d, J = 7.4, 1H, H3), 7.03 (t, J = 7.4, 1H, H4 or H5), 5.88 (d, J = 7.3, 1H, H6), 5.71 (s, 10H, Cp), 1.97 (s, 3H, Me). ^{13}C{gated-^{1}H} NMR (C_6D_5Cl, 23 °C): δ 198.3 (s, C1), 147.2 (s, C2), 132.4 (d, J = 159, C4), 129.2 (d, J = 155, C3), 126.3 (d, J = 161, C5), 112.9 (d, J = 177, Cp), 103.3 (dd, J = 131, 9, C6), 23.6 (qd, J = 126, 4, Me).

Generation of $[Cp_2Hf\{C(SiMe_3){=}C(Me)(o\text{-tolyl})\}][B(C_6F_5)_4]$. A solution of **2f·$C_6D_5Cl$** in C_6D_5Cl was generated in an NMR tube as described above and cooled to −196 °C, and $MeC{\equiv}CSiMe_3$ (2 equiv) was added by vacuum transfer. The tube was warmed to 23 °C for 15 min, giving an orange solution. NMR and ESI-MS analysis confirmed that insertion was complete. ^{1}H NMR (C_6D_5Cl, 23 °C): δ 7.43 (dd, J = 6.1, 1.4, 1H, aryl), 7.22 (d, J = 7.6, 1H, aryl), 6.37 (t, J = 6.7, 1H, aryl), 6.08 (br m, 1H, aryl), 5.70 (br s, 10H, Cp), 2.08 (s, 3H, *o*-Me), 1.79 (s, 3H, ═C*Me*), −0.01 (s, 9H, ═CSi*Me*$_3$). ^{13}C{^{1}H} NMR (C_6D_5Cl, 23 °C): δ 216.5 (Hf*C*═), 149.1, 147.9, 142.9, 140.2, 132.9, 130.8, 114.9 (Cp), 101.5 (═*C*MeAr), 26.1 (*o*-Me), 20.2 (═C*Me*), 1.4 (═CSi*Me*$_3$). ESI-MS (C_6D_5Cl) $[Cp_2Hf(C(SiMe_3){=}C(Me)(o\text{-tolyl}]^+$: calcd m/z 513.2, found 513.0.

Generation of $[Cp_2Hf(Ph)(ClC_6D_5)][B(C_6F_5)_4]$ (2g·C_6D_5Cl). An NMR tube was charged with Cp_2HfPh_2 (20.0 mg, 0.0432 mmol) and $[C_6Me_6H][B(C_6F_5)_4]$ (36.4 mg, 0.0432 mmol), and C_6D_5Cl was added by vacuum transfer at −196 °C. The tube was warmed to 23 °C with vigorous agitation, resulting in a pale yellow solution. NMR analysis after 15 min at 23 °C showed clean formation of **2g·C_6D_5Cl**, 1 equiv benzene, and 1 equiv of C_6Me_6. ^{1}H NMR (C_6D_5Cl, 23 °C): δ 7.31 (t, J = 7.5, 2H, *m*-Ph), 7.17 (m, 3H, *o*-, *p*-Ph), 5.90 (s, 10H, Cp). ^{13}C{^{1}H} NMR (C_6D_5Cl, 23 °C): δ 192.8 (s, *ipso*-Ph), 135.2 (d, J = 155, *o*-Ph), 129.1 (coupling obscured by solvent peak, *p*-Ph), 128.6 (d, J = 162, *m*-Ph), 115.4 (d, J = 177, Cp).

Generation of $[Cp_2Hf\{C(SiMe_3){=}C(Me)Ph\}][B(C_6F_5)_4]$. A solution of **2g·$C_6D_5Cl$** in C_6D_5Cl was generated in an NMR tube as described above and cooled to −196 °C, and $MeC{\equiv}CSiMe_3$ (30 μmol) was added by vacuum transfer. The tube was warmed to 23 °C and agitated, giving a yellow solution. The solvent was removed under vacuum. The solid was dried under vacuum for 30 min, and fresh C_6D_5Cl (0.6 mL) was added by vacuum transfer. NMR and ESI-MS analysis confirmed that insertion was complete. ^{1}H NMR (C_6D_5Cl, 23 °C): δ 7.28 (d, J = 6.5, 2H, *o*-Ph), 7.15 (t, partially obscured by solvent, *p*-Ph), 6.97 (t, J = 7.4, partially obscured by solvent, *m*-Ph), 5.74 (s, 10H, Cp), 1.89 (s, 3H, Me), −0.03 (s, 9H, $SiMe_3$). ^{13}C{^{1}H} NMR (C_6D_5Cl, 23 °C): δ 216.3 (Hf−C), 152.7 (Ph), 150.5 (Ph), 138.0 (Ph), 131.9 (Ph), 115.3 (Cp), 113.7 (═*C*MePh), 25.8 (Me), 1.4 ($SiMe_3$). ESI-MS (C_6D_5Cl) $[Cp_2Hf(C(SiMe_3){=}C(Me)(Ph)]^+$: calcd m/z 499.1, found 499.0.

$[C_6Me_6(CD_2Cl)][Zr_2Cl_9]$ (4). The nondeuterated analogue of **4**, $[C_6Me_6(CH_2Cl)][Zr_2Cl_9]$, was previously characterized by X-ray and elemental analysis.[14] An NMR tube was charged with C_6Me_6 (11.6 mg, 0.0715 mmol) and $ZrCl_4$ (33.3 mg, 0.143 mmol), and CD_2Cl_2 (0.9 mL) was added by vacuum transfer at −78 °C. The tube was warmed to 40 °C for 3 h, giving a suspension of a white solid in a yellow supernatant. ^{1}H NMR (CD_2Cl_2): δ 2.91 (s, 3H), 2.69 (s, 6H), 2.41 (s, 6H), 1.55 (s, 3H). ^{13}C{^{1}H} NMR (CD_2Cl_2): δ 194.6, 194.5, 142.3, 61.5, 46.7 (1-2-3-2-1 pentet, $J_{CD} = 27$ Hz), 26.2, 24.1, 22.3, 16.7. ESI-MS (C_6D_5Cl) $[C_6Me_6(CD_2Cl)]^+$: calcd *m*/*z* 213.1, found 213.0.

Generation of $[\{Cp_2ZrPh\}_2(\mu\text{-}Cl)][B(C_6F_5)_4]$ (5). An NMR tube was charged with $[Cp_2ZrPh][B(C_6F_5)_4]\cdot(C_6H_6)_{2.6}$ (28.2 mg, 23.9 μmol) and $[NBu_3CH_2Ph]Cl$ (3.7 mg, 12 μmol), and CD_2Cl_2 was added by vacuum transfer at −78 °C. The tube was vigorously agitated at 23 °C until the solids dissolved to give a colorless solution. ^{1}H NMR (CD_2Cl_2, −89 °C): δ 7.16 (d, $J = 6.6$, 4H, *o*-Ph), 7.07 (m, 6H, *m*- and *p*-Ph), 6.30 (s, 20H, Cp). ^{13}C{^{1}H} (CD_2Cl_2, −89 °C): δ 185.2 (*ipso*-Ph), 132.3 (*o*-Ph), 127.3 (*p*-Ph), 126.8 (*m*-Ph), 115.0 (Cp).

Generation of $[\{Cp_2HfPh\}_2(\mu\text{-}Cl)][B(C_6F_5)_4]$ (6). An NMR tube was charged with Cp_2HfPh_2 (3.3 mg, 0.0071 mmol) and $[C_6Me_6H][B(C_6F_5)_4]$ (6.5 mg, 0.0077 mmol), and CD_2Cl_2 (0.6 mL) was added by vacuum transfer at −196 °C. The tube was warmed to −78 °C and agitated to give a pale yellow solution. NMR analysis after 30 min at −78 °C showed clean formation of **6**, 1 equiv of benzene, 0.5 equiv of **4**, and 0.5 equiv of C_6Me_6. Data for **6**: ^{1}H NMR (CD_2Cl_2, −80 °C): δ 7.31 (d, $J = 8.1$, 4H, *o*-Ph), 7.19 (t, $J = 7.5$, 4H, *m*-Ph), 7.10 (t, $J = 7.4$, 2H, *p*-Ph), 6.26 (s, 20H, Cp). ^{13}C{^{1}H} NMR (CD_2Cl_2, −80 °C): δ 188.6 (*ipso*-Ph), 136.7 (*o*-Ph), 127.1 (*m*-Ph), 114.5 (Cp). The *p*-Ph resonance is obscured by the benzene peak.

Generation of $[Cp'_2Zr(Ph)(THF)][B(C_6F_5)_4]$ (7). A solution of **2f·C_6D_5Cl** in C_6D_5Cl was generated in an NMR tube and cooled to −196 °C, and THF (4 equiv) was added by vacuum transfer. The tube was warmed to 23 °C, giving a pale yellow solution. The volatiles were removed under vacuum. The pale yellow solid was washed with hexane (1 mL) and benzene (2 × 1 mL), triturated with CD_2Cl_2 (0.2 mL), and dissolved in CD_2Cl_2 (0.6 mL), and NMR spectra were recorded. ^{1}H NMR (CD_2Cl_2, −89 °C): δ 7.23 (t, $J =$ 7, 2H, *m*-Ph), 7.13 (t, $J = 7$, 1H, *p*-Ph), 7.09 (d, $J = 7$, 2H, *o*-Ph), 6.44 (br s, 2H, Cp′ CH), 6.27 (br s, 2H, Cp′ CH), 6.23 (br s, 2H, Cp′ CH), 6.01 (br s, 2H, Cp′ CH), 4.04 (m, 4H, THF), 2.08 (m, 4H, THF), 1.83 (s, 6H, Cp′ Me). ^{13}C{gated-^{1}H} NMR (CD_2Cl_2, −89 °C): δ 186.5 (s, *ipso*-Ph), 131.5 (d, $J = 151$, *o*-Ph), 129.6 (s, Cp′ *ipso*), 127.6 (d, $J = 160$, *m*-Ph), 126.9 (d, $J = 161$, *p*-Ph), 117.8 (d, $J = 174$, Cp′ CH), 113.7 (d, $J = 176$, Cp′ CH), 113.6 (d, $J = 176$, Cp′ CH), 112.3 (d, $J = 173$, Cp′ CH), 79.3 (t, $J = 155$, THF), 25.4 (t, $J = 135$, THF), 14.7 (q, $J = 129$, Cp′ Me).

$Cp_2Zr(Ph)Cl$ (8). An NMR tube was charged with $[Cp_2ZrPh][B(C_6F_5)_4]\cdot(C_6H_6)_{2.6}$ (**2d**, 20 mg, 17 μmol) and $[NBu_3CH_2Ph]Cl$ (5.3 mg, 17 μmol), and CD_2Cl_2 was added by vacuum transfer at −78 °C. The tube was vigorously agitated at 23 °C until all of the solids dissolved to give a colorless solution. ^{1}H NMR (CD_2Cl_2, −89 °C): δ 7.14 (d, $J = 7.1$, 2H, *o*-Ph), 7.02 (t, $J = 7.3$, 2H, *m*-Ph), 6.94 (t, $J = 7.2$, 1H, *p*-Ph), 6.29 (s, 10H, Cp). ^{13}C{gated-^{1}H} (CD_2Cl_2, −89 °C): δ 182.3 (s, *ipso*-Ph), 136.5 (d, $J = 157$, *o*-Ph), 126.4 (d, $J = 158$, *m*-Ph), 124.2 (*p*-Ph), 113.5 (d, $J = 175$, Cp).

Computational Methods. Structures were optimized using the Gaussian 03 software package using density functional theory (DFT).[33] The geometry optimizations were performed using the BP86[34] density functional. All main group atoms were modeled using the 6-31G* basis set.[35] Zirconium was modeled using the LANL2DZ basis set including an effective core potential.[36] Hafnium was modeled using the SDD basis set with a small effective core potential replacing 60 core electrons. Calculations of reference compounds established that this methodology correctly predicts the structures of chlorocarbon complexes and the presence of agostic interactions (see Supporting Information). Energies are reported without zero-point corrections. Figures of optimized geometries were drawn using the MOLEKEL software package.[37]

Acknowledgment. This work was supported by the National Science Foundation (CHE-0516950). We acknowledge the Burroughs Welcome Fund Interfaces Cross-Disciplinary Training Program at the University of Chicago for partial support of the computer cluster. We thank Jeffery R. Hammond for helpful discussions.

Supporting Information Available: Details concerning the choice and validation of the computational methods and additional computational results (pdf). This material is available free of charge via the Internet at http://pubs.acs.org.

OM700436Z

(33) Frisch, M. J.; et al. *Gaussian 03*, Revision C.02. See the Supporting Information for the complete citation.

(34) (a) Becke, A. D. *Phys. Rev. A* **1988**, *38*, 3098. (b) Vosko, S. H.; Wilk, L.; Nusair, M. *Can. J. Phys.* **1980**, *58*, 1200. (c) Perdew, J. P. *Phys. Rev. B* **1986**, *33*, 8822.

(35) (a) Rassolov, V. A.; Ratner, M. A.; Pople, J. A.; Redfern, P. C.; Curtiss, L. A. *J. Comput. Chem.* **2001**, *22*, 976. (b) Rassolov, V. A.; Pople, J. A.; Ratner, M. A.; Windus, T. L. *J. Chem. Phys.* **1998**, *109*, 1223. (c) Ditchfield, R.; Hehre, W. J.; Pople, J. A. *J. Chem. Phys.* **1971**, *54*, 724.

(36) (a) Hay, P. J.; Wadt, W. R. *J. Chem. Phys.* **1985**, *82*, 270. (b) Wadt, W. R.; Hay, P. J. *J. Chem. Phys.* **1985**, *82*, 284. (c) Hay, P. J.; Wadt, W. R. *J. Chem. Phys.* **1985**, *82*, 299.

(37) Flükiger, P.; Lüthi, H. P.; Portmann, S.; Weber, J. *MOLEKEL 4.3*; Swiss Center for Scientific Computing: Manno, Switzerland, 2000−2002. Portmann, S.; Lüthi, H. P. MOLEKEL: An Interactive Molecular Graphics Tool. *Chimia* **2000**, *54*, 766−770.